The nature of the DX state in Ge-doped AlGaN

Cite as: Appl. Phys. Lett. **116**, 222102 (2020); https://doi.org/10.1063/5.0008362 Submitted: 21 March 2020 . Accepted: 26 May 2020 . Published Online: 03 June 2020

Pegah Bagheri , Ronny Kirste, Pramod Reddy , Shun Washiyama , Seiji Mita, Biplab Sarkar , Ramón Collazo, and Zlatko Sitar







ARTICLES YOU MAY BE INTERESTED IN

Variable range hopping mechanism and modeling of isolation leakage current in GaN-based high-electron-mobility transistors

Applied Physics Letters 116, 222101 (2020); https://doi.org/10.1063/5.0004957

Impact of defects on Auger recombination in c-plane InGaN/GaN single quantum well in the efficiency droop regime

Applied Physics Letters 116, 222106 (2020); https://doi.org/10.1063/5.0004321

Shallow Si donor in ion-implanted homoepitaxial AIN

Applied Physics Letters 116, 172103 (2020); https://doi.org/10.1063/1.5144080

Lock-in Amplifiers up to 600 MHz







The nature of the DX state in Ge-doped AlGaN

Cite as: Appl. Phys. Lett. **116**, 222102 (2020); doi: 10.1063/5.0008362 Submitted: 21 March 2020 · Accepted: 26 May 2020 · Published Online: 3 June 2020







Pegah Bagheri,^{1,a)} (D) Ronny Kirste,² Pramod Reddy,² (D) Shun Washiyama,¹ (D) Seiji Mita,² Biplab Sarkar,¹ (D) Ramón Collazo,¹ and Zlatko Sitar^{1,2} (D)

AFFILIATIONS

- ¹Department of Materials Science and Engineering, North Carolina State University, Raleigh, North Carolina 27695, USA ²Adroit Materials, Cary, North Carolina 27518, USA
- ^{a)}Author to whom correspondence should be addressed: pbagher@ncsu.edu

ABSTRACT

Electrical conductivity in high Al-content AlGaN has been severely limited, presumably due to a DX transition forming an acceptor state and subsequent self-compensation, which imposed an upper limit on the achievable free carrier concentration. To elucidate this idea, this paper examines Ge doping as a function of Al-content in AlGaN and finds a different behavior: for Al compositions below 40%, Ge behaved as a shallow donor with an ionization energy below 20 meV, while for Al compositions above 40%, above DX transition, it emerged as a deep donor. The ionization energy of this deep state increased with increasing Al content and reached 150 meV for 60% AlGaN. Around the DX transition, a continuous change from the shallow to deep donor was observed. In contrast to the density functional theory predictions, acceptor-type states corresponding to a DX-type transition were not observed. This finding may have profound technological consequences for the development of AlGaN- and AlN-based devices as it offers a feasible pathway to high n-conductivity in these compounds.

Published under license by AIP Publishing. https://doi.org/10.1063/5.0008362

Controllable n-type doping in wide and ultra-wide bandgap III-nitrides, GaN, AlN, and their alloys, is crucial for UV optoelectronic, power electronic, and potential plasmonic devices. $^{1-5}$ Si is an established shallow n-type dopant in GaN and $Al_xGa_{1-x}N$ (x<0.8). $^{6-8}$ However, an increased ionization energy is observed for Si in $Al_xGa_{1-x}N$ (for x>0.8) that is commonly attributed to the formation of a DX center, consequently limiting the achievable conductivity in high Al content AlGaN. $^{6,8-10}$ An additional challenge associated with Si doping is the observation of tensile stress in high dislocation density, heavily doped films due to the Fermi level effect, which drives the vacancy-mediated dislocation climb at carrier concentrations above $10^{19}\,\mathrm{cm}^{-3}\,^{11,12}$

Similar to Si, Ge is energetically favorable to be substituted on the metal site than the nitrogen site in n-type AlGaN and acting as a donor. However, it could potentially provide several advantages over Si as a donor dopant in III-nitrides. There are various reports of crackfree, heavily Ge-doped AlGaN and GaN epitaxial layers grown on sapphire with carrier concentrations exceeding 10²⁰ cm⁻³, suggesting that Ge doping allows for high doping with no significant tensile stress. However, Ge is also expected to undergo a DX transition in AlGaN. Theoretical work by Gordon *et al.* predicts such onset of the Ge-related DX formation to be at Al content of around 50%. Understanding and controlling DX in AlGaN is technologically crucial since it can open up a pathway for high conductivity Al-rich AlGaN

by Ge doping. To identify this DX transition, one of the easily recognizable characteristics is an apparent increase in the ionization energy. 9.18 Although Ge has been considered as a potential donor in III-nitrides, its behavior as a donor and related compensation mechanisms, such as DX formation and self-compensation, have not been established experimentally. As a first step in determining the possibility of using Ge as a technical dopant in AlGaN, it is necessary to experimentally confirm the predicted DX transition and determine its onset.

Beyond practical applicability as a shallow donor, Ge also provides an opportunity to bring about new understanding of the DX formation within III-nitrides. Based on current understanding, a donor impurity undergoes a DX transformation when the dopant experiences bond "rupturing," resulting in an off-site relaxation of the donor atom and formation of a deep acceptor, which forms an acceptor (DX^{-1}) —donor (d^+) pair, i.e., a thermodynamic transition where the DX^- and d^+ concentrations self-adjust to "pin" the Fermi level to the (-1/+1) transition energy. According to this hypothesis, forming a DX center is a type of self-compensation where the carrier concentration increases with the increase in doping concentration until a critical concentration has been reached. At this point, the Fermi level reaches the (-1/+1) transition energy, beyond which the free carrier concentration remains constant despite an increase in the doping concentration. There are various reports attempting to characterize DX nature

in Si doped AlGaN and AlN by using persistent photoconductivity and electron paramagnetic resonance. ^{19,20} However, there are inconsistencies in the literature both experimentally and theoretically and DX nature in n-type AlGaN is still under debate. ^{9,21,22} Since Ge is predicted to form a DX transition in AlGaN at a lower Al content, it presents a more convenient way to study the electronic nature of the DX center in comparison to Si, which forms a measurable DX center only for Al content >0.9. However, for Al-rich AlGaN other challenges, such as Ohmic contacts and increased vacancy related compensation, also play a significant role. ^{7,23}

In this work, Ge-doped AlGaN films with varying Al content and constant dopant concentration were grown via metal-organic chemical vapor deposition (MOCVD). Temperature-dependent Hall effect measurements were used to determine free carrier concentration, mobility, and Ge ionization energy to elucidate on the DX center formation and its electronic nature.

All AlGaN films were grown on 2", c-oriented sapphire wafers in a vertical, rf-heated, low-pressure (20 Torr) MOCVD reactor, using triethylgallium (TEG), trimethylaluminum (TMA), and ammonia as gallium, aluminum, and nitrogen precursors, respectively. Prior to the growth, the sapphire wafers were annealed within the reactor in $\rm H_2$ at 1100 °C for 7 min and then nitrided in a 1:1 ammonia–hydrogen mixture at 950 °C for 4 min. A low temperature, at 650 °C, AlN buffer layer was deposited prior to the growth of a 200 nm thick AlN layer at 1200 °C that served as an Al-polar AlN template. Subsequently, 500 nm thick Ge-doped AlGaN layers with varying Al-content between 0 and 60% were grown, using a 1000 ppm germane mixture in nitrogen as the Ge precursor for the targeted Ge concentration of 2 × 10¹⁹ cm⁻³. The AlGaN layers were grown under $\rm N_2$ diluent, at growth temperature of 950 °C, and V/III of 3200; these parameters corresponded to a supersaturation of 50 000.

The AlGaN composition, residual stress, and dislocation density were determined by x-ray diffraction (XRD) measurements using a Philips X'Pert materials research diffractometer with a Cu anode and using methods described elsewhere.²⁴ An ION-TOF time-of-flight secondary ion mass spectrometer (TOF-SIMS) was used to determine the Ge concentration in AlGaN films. The acquisition conditions for the non-interlaced sputtering mode used for the measurement were described elsewhere.²⁵ Germanium concentration was determined under a negative ion detection mode and calibrated against an ionimplanted Al_{0.3}Ga_{0.7}N standard. The aluminum/gallium ratio was determined following the procedure explained elsewhere.²⁶ Ohmic contacts were realized on all AlGaN films by evaporation and rapid thermal annealing of V/Al/Ni/Au metal stacks.²⁷ Electrical characterization was performed using temperature-dependent Hall measurements (Ecopia HMS-5500) in the Van der Pauw configuration and in a temperature range of 160-700 K. According to SIMS, Ge concentration for different compositions varies from $1.5 \times 10^{19} \, \text{cm}^{-3}$ to about $3 \times 10^{19} \, \mathrm{cm}^{-3}$ while it was targeted at $2 \times 10^{19} \, \mathrm{cm}^{-3}$ shown in Table I. This may affect the measurable carrier concentrations and mobility slightly. To correct for small deviations between the nominal and actual Ge concentrations as determined by SIMS, all carrier concentration and mobility measurements were normalized to the nominal Ge tion and mobility measurements were normalized concentration value of $2 \times 10^{19} \, \text{cm}^{-3}$ (i.e., $\times \frac{[\text{Ge}]_{\text{nominal}}}{[\text{Ge}]_{\text{actual}}}$ for carrier concentration).

X-ray diffraction measurements confirmed that the intended Al-content in AlGaN. All AlGaN films were relaxed with (302)

TABLE I. Ge concentration determined by SIMS for each Al composition.

Al composition (%)	Ge concentration by SIMS (cm ⁻³)
1	1.5×10^{19}
7	2×10^{19}
17	2×10^{19}
27	2×10^{19}
40	3×10^{19}
50	3×10^{19}
60	3×10^{19}

 ω -rocking curve FWHMs ranging from 2000 to 2300 arc sec, corresponding to a total dislocation density of $\sim 10^{10}\,\mathrm{cm}^{-2}$. Contacts showed Ohmic behavior for all AlGaN compositions and temperatures, as demonstrated by linear current–voltage characteristics. As an example, Fig. 1 shows I-V characteristics for 40, 50, and 60% Ge:AlGaN films obtained at room temperature.

Since Ge is a group IV substitutional impurity to either Ga or Al sites, it is expected to be a shallow hydrogenic-type donor with an ionization energy of 29 and 75 meV for GaN and AlN, respectively. This should yield measurable room temperature carrier concentrations in AlGaN over a wide range of Al contents. Figure 2 shows room temperature conductivity, carrier concentration, and mobility for Ge:AlGaN as a function of Al content as determined by Hall measurements. One can see that for Al contents <40%, the free carrier concentration remains more or less constant, indicating a low ionization energy and low compensation, i.e., no significant concentration of DX centers or other compensators, like $C_{\rm N}$ or Ge-vacancy complexes.

However, when the Al-content is increased beyond 40%, both carrier concentration and conductivity decrease sharply by more than two orders of magnitude. The drop in the conductivity for x > 40% agrees well with the decrease in slopes of I-V curves shown in Fig. 1. Simultaneously, the mobility collapses to the low single digit values, suggesting a high concentration of ionized point defects. This abrupt change seems to be consistent with the formation of the Ge-related

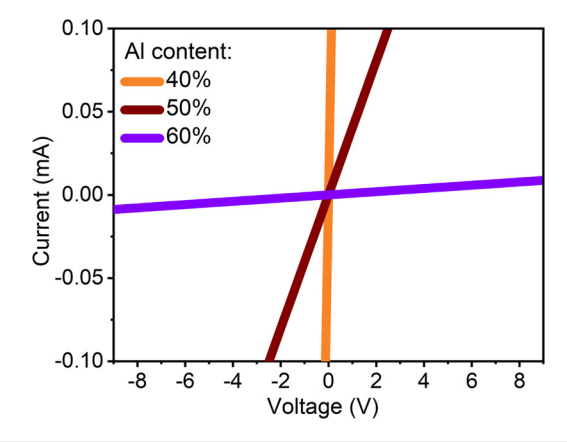


FIG. 1. Room temperature *I*–V characteristics of Ge:AlGaN for 40, 50, and 60% Al content showing Ohmic contact behavior.

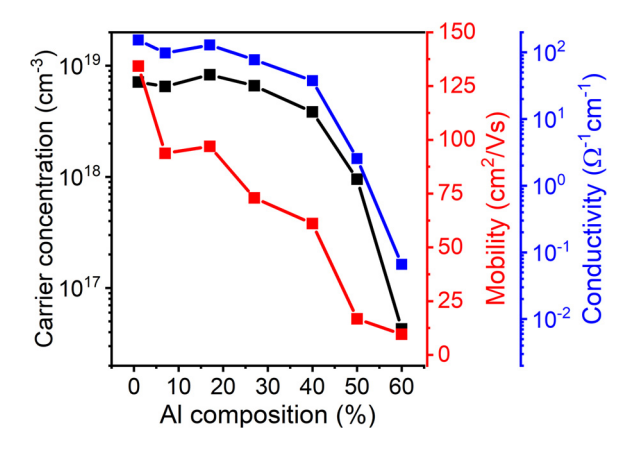


FIG. 2. Room temperature carrier concentration, conductivity, and mobility of Ge:AlGaN as a function of the Al content with a constant Ge concentration of $2 \times 10^{19} \, \text{cm}^{-3}$.

DX center, which was predicted to occur around 50% Al-content in prior density functional theory (DFT) work.⁹

Figure 3 shows free carrier concentration as a function of temperature for various AlGaN compositions. For x < 40%, ionization energy was estimated as the activation energy considering negligible compensation since they are degenerately doped alloys. However, for x > 40%, the ionization energy, E_D , was extracted as the best fit of the charge balance equation for one acceptor and one donor, assuming a complete ionization of the acceptors $(N_A = N_A^-)^{28}$

$$n + N_A = \frac{N_D}{1 + \frac{2}{N_c(T)} n \exp\left(\frac{E_D}{kT}\right)}.$$
 (1)

Here, N_A , N_D , and N_C are acceptor and donor concentrations, and effective conduction band density of states, respectively; E_D is the donor ionization energy, while n is the free electron concentration.

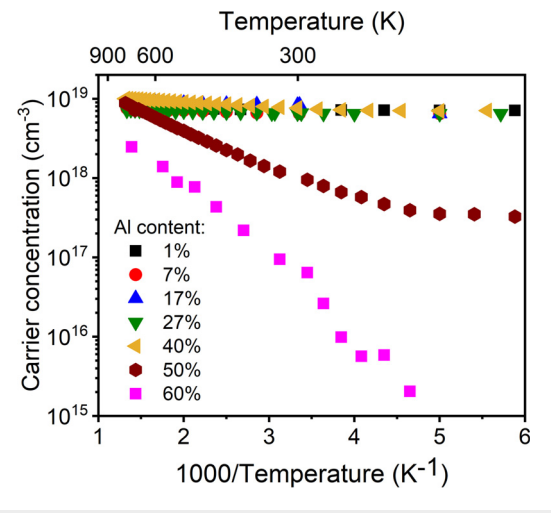


FIG. 3. Temperature-dependent free carrier concentration for different AlGaN compositions with a constant Ge concentration of 2×10^{19} cm⁻³.

 N_C for AlGaN was estimated from the effective conduction band densities of states for GaN and AlN using the following equation:²⁹

$$N_C(Al_xGa_{1-x}N) = xN_C(AlN) + (1-x)N_C(GaN).$$
 (2)

As seen in Fig. 3, no significant change in the carrier concentration with temperature was observed for the Al content below 40%, indicating a hydrogenic-like donor with a low ionization energy and negligible compensation. Interestingly, for samples with Al content greater than 40%, a second slope appeared at higher temperatures, suggesting a second donor with a higher ionization energy. At high temperatures, the carrier concentration showed a saturation level similar to that observed for the lower Al content AlGaN indicative of a high ionization level of the deep donor. For the highest Al content alloy, only a single slope corresponding to the highest ionization energy among all the compositions was observed.

Figure 4 shows ionization energies of the two donor states extracted from the temperature dependent measurements. The shallow donor exhibited a low ionization energy, consistent with the hydrogenic model, which increased only slightly with the Al content in AlGaN. In contrast, the ionization energy of the deep donor was significantly higher, increasing rapidly with the increasing Al content, and reached 150 meV at an Al content of 60%.

The abundance of each state seemed to depend on the AlGaN composition as well, with the fraction of the deep donor state increasing with the Al content. The population distribution between the shallow and deep donor states for each AlGaN composition was estimated from Fig. 3. For the AlGaN with 40%, 50%, and 60% Alcontent, the fraction of Ge atoms in the shallow donor state changed from 100% to 0.4% to $\sim\!\!0\%$, respectively. A clear transition from the shallow donor (<30 meV) to deep donor (>110 meV) occurred at around 50% Al content. For AlGaN with Al content >50%, one can expect that practically all Ge dopants will be in the deep donor state that has a high ionization energy and will produce very low conductivity.

From these results, we can draw some fundamental conclusions about the nature of the Ge DX center in AlGaN. Considering the charge balance equation that includes multiple donors and acceptors,

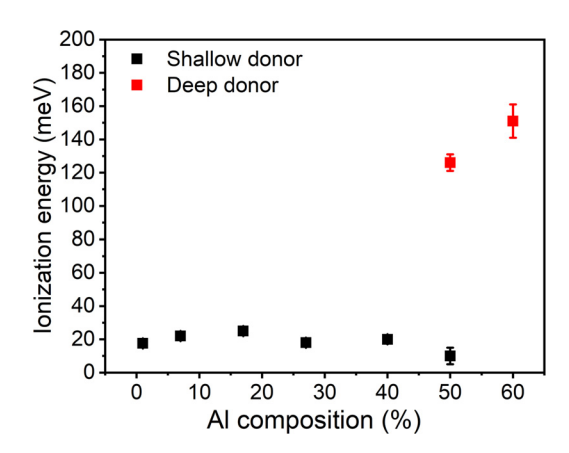


FIG. 4. Ionization energy of the shallow and deep donor states as a function of AlGaN composition. Ge concentration was kept constant at $2 \times 10^{19} \, \mathrm{cm}^{-3}$. The error bars show the 95% confidence range for the fitting parameters.

the only reasonable explanation for the observed temperature dependence of the free carrier concentration with two slopes is the presence of two donor states, one with low and the other with high ionization energy. Population of Ge atoms in each state in equilibrium depends on the AlGaN composition. It has to be noted that none of the other possible cases, like a shallow donor and a fully ionized acceptor, or a shallow donor and a deep acceptor, can replicate the observed temperature-dependent behavior. Figure 5 compares the calculated carrier concentration as a function of temperature for the above three scenarios. A 10 meV shallow donor ionization energy was considered and a variation from 100 meV to 200 meV of the deep level ionization energy for 50% and 60% Al compositions, respectively. Based on the charge balance equation for the above cases, if Ge was considered as a shallow acceptor upon the formation of the DX state, it will act as a compensator, and no significant change in the activation energy of the shallow state will be observed [Fig. 5(a)]. If Ge formed a deep acceptor state, showing an increase in the ionization energy by increasing the Ge atomic fraction in the deep level, one would expect a uniform increase in the slope in the carrier concentration curves but not two slopes [Fig. 5(b)]. Only a distribution of Ge atoms between a shallow and deep donor state will show two ionization energies, as shown in Fig. 5(c). Comparing these three cases to the result in Fig. 3, one can see that only the third scenario, Fig. 5(c), reproduces the experimental results.

Based on these observations, we propose a model to describe the DX electronically. Although our experimental observations are in a reasonable agreement with DFT analyses, which hypothesize a DX center in Ge-doped AlGaN forming for Al compositions greater than 50% and an ionization energy that increases with the increase in Al content, the typical interpretation of the DX as a (-1/+1) transition energy cannot explain the observation of a distribution of shallow and deep donor states. Instead, the transition to compositions with DX centers corresponded to the emergence of a deep donor (DX) characterized by the (0/+1) transition whose concentration (and atomic fraction of Ge in DX state) and ionization energy increase with Al content. This is an important observation and departure from the current understanding since the typical interpretation of the (-1/+1) transition, which pins the Fermi level at the transition energy, severely limits the achievable conductivity through a self-compensation process. However, if the DX is a deep donor, high conductivity may be achieved by doping to very high concentrations and the likely limitation is from increased compensation from vacancy-donor complexes at higher doping concentrations, which can be managed.

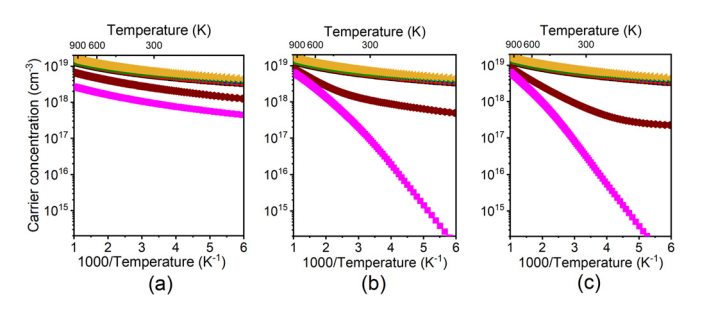


FIG. 5. Calculated carrier concentrations with temperature assuming: (a) one shallow donor and one fully ionized acceptor, (b) one shallow donor and one deep acceptor, and (c) two donors with ionization energies obtained from Fig. 4.

In conclusion, the behavior of the Ge dopant in AlGaN was studied as a function of Al-content in the alloy. At Al compositions below 40%, it behaved as a shallow donor with ionization energy below 20 meV. At Al compositions above 40%, it emerged as a deep donor, whose ionization energy increased with increasing Al content and reached 150 meV for AlGaN with 60% Al. At this point, only the deep donor state was observed. In contrast to the DFT predictions, acceptor-type states were not observed. Based on these studies, we propose the DX as a deep donor (0/+1) transition, whose ionization energy increases with Al content, rather than a Fermi-level-pinning (-1/+1) transition. This understanding has profound technological consequences as it offers a feasible pathway to high n-conductivity in AlGaN and even AlN.

The authors gratefully acknowledge funding in part from AFOSR (Nos. FA9550-17-1-0225 and FA9550-19-1-0114), NSF (Nos. ECCS-1916800, ECCS-1508854, ECCS-1610992, DMR-1508191, and ECCS-1653383), ARO (Nos. W911NF-15-2-0068, W911NF-16-C-0101, and W911NF-18-1-0415), and DOE (No. DE-SC0011883). We also thank Marc P. Hoffmann for support of this project.

DATA AVAILABILITY

The data that support the findings of this study are available within the article.

REFERENCES

- ¹R. Kirste, N. Rohrbaugh, I. Bryan, Z. Bryan, R. Collazo, and A. Ivanisevic, Annu. Rev. Anal. Chem. **8**, 149 (2015).
- ²R. Kirste, M. P. Hoffmann, E. Sachet, M. Bobea, Z. Bryan, I. Bryan, C. Nenstiel, A. Hoffmann, J.-P. Maria, R. Collazo, and Z. Sitar, Appl. Phys. Lett. 103, 242107 (2013).
- ³J. Xie, S. Mita, Z. Bryan, W. Guo, L. Hussey, B. Moody, R. Schlesser, R. Kirste, M. Gerhold, R. Collazo, and Z. Sitar, Appl. Phys. Lett. **102**, 171102 (2013).
- ⁴K. A. Jones, T. P. Chow, M. Wraback, M. Shatalov, Z. Sitar, F. Shahedipour, K. Udwary, and G. S. Tompa, J. Mater. Sci. 50, 3267 (2015).
- 5J. Y. Tsao, S. Chowdhury, M. A. Hollis, D. Jena, N. M. Johnson, K. A. Jones, R. J. Kaplar, S. Rajan, C. G. Van de Walle, E. Bellotti, C. L. Chua, R. Collazo, M. E. Coltrin, J. A. Cooper, K. R. Evans, S. Graham, T. A. Grotjohn, E. R. Heller, M. Higashiwaki, M. S. Islam, P. W. Juodawlkis, M. A. Khan, A. D. Koehler, J. H. Leach, U. K. Mishra, R. J. Nemanich, R. C. N. Pilawa-Podgurski, J. B. Shealy, Z. Sitar, M. J. Tadjer, A. F. Witulski, M. Wraback, and J. A. Simmons, Adv. Electron. Mater. 4, 1600501 (2018).
- ⁶R. Collazo, S. Mita, J. Xie, A. Rice, J. Tweedie, R. Dalmau, and Z. Sitar, Phys. Status Solidi C 8, 2031 (2011).
- 7I. Bryan, Z. Bryan, S. Washiyama, P. Reddy, B. Gaddy, B. Sarkar, M. Hayden Breckenridge, Q. Guo, M. Bobea, J. Tweedie, S. Mita, D. Irving, R. Collazo, and Z. Sitar, Appl. Phys. Lett. 112, 062102 (2018).
- ⁸B. Borisov, V. Kuryatkov, Y. Kudryavtsev, R. Asomoza, S. Nikishin, D. Y. Song, M. Holtz, and H. Temkin, Appl. Phys. Lett. **87**, 132106 (2005).
- ⁹L. Gordon, J. L. Lyons, A. Janotti, and C. G. Van de Walle, Phys. Rev. B 89, 085204 (2014).
- ¹⁰M. S. Brandt, R. Zeisel, S. T. B. Gönnenwein, M. W. Bayerl, and M. Stutzmann, Phys. Status Solidi B 235, 13 (2003).
- ¹¹J. Xie, S. Mita, A. Rice, J. Tweedie, L. Hussey, R. Collazo, and Z. Sitar, Appl. Phys. Lett. 98, 202101 (2011).
- ¹²J. S. Harris, J. N. Baker, B. E. Gaddy, I. Bryan, Z. Bryan, K. J. Mirrielees, P. Reddy, R. Collazo, Z. Sitar, and D. L. Irving, Appl. Phys. Lett. 112, 152101 (2018)
- ¹³C. G. Van de Walle and J. Neugebauer, J. Appl. Phys. **95**, 3851 (2004).
- ¹⁴C. B. Lim, A. Ajay, J. Lähnemann, C. Bougerol, and E. Monroy, Semicond. Sci. Technol. 32, 125002 (2017).

- ¹⁵A. Dadgar, J. Bläsing, A. Diez, and A. Krost, Appl. Phys. Express 4, 011001 (2011).
- ¹⁶C. Nenstiel, M. Bügler, G. Callsen, F. Nippert, T. Kure, S. Fritze, A. Dadgar, H. Witte, J. Bläsing, A. Krost, and A. Hoffmann, Phys. Status Solidi RRL 9, 716 (2015).
- 17 R. Blasco, A. Ajay, E. Robin, C. Bougerol, K. Lorentz, L. C. Alves, I. Mouton, L. Amichi, A. Grenier, and E. Monroy, J. Phys. Appl. Phys. 52, 125101 (2019).
- ¹⁸A. Bansal, K. Wang, J. S. Lundh, S. Choi, and J. M. Redwing, Appl. Phys. Lett. 114, 142101 (2019).
- ¹⁹R. Zeisel, M. W. Bayerl, S. T. B. Goennenwein, R. Dimitrov, O. Ambacher, M. S. Brandt, and M. Stutzmann, Phys. Rev. B 61, R16283 (2000).
- ²⁰K. Irmscher, T. Schulz, M. Albrecht, C. Hartmann, J. Wollweber, and R. Fornari, Physica B 401–402, 323 (2007).
- ²¹C. G. Van de Walle, Phys. Rev. B 57, R2033 (1998).
- 22N. T. Son, M. Bickermann, and E. Janzén, Appl. Phys. Lett. 98, 092104 (2011).
- ²³B. Sarkar, S. Mita, P. Reddy, A. Klump, F. Kaess, J. Tweedie, I. Bryan, Z. Bryan, R. Kirste, E. Kohn, R. Collazo, and Z. Sitar, Appl. Phys. Lett. 111, 032109 (2017).

- ²⁴J. Tweedie, R. Collazo, A. Rice, J. Xie, S. Mita, R. Dalmau, and Z. Sitar, J. Appl. Phys. 108, 043526 (2010).
- 25A. Klump, C. Zhou, F. A. Stevie, R. Collazo, and Z. Sitar, J. Vac. Sci. Technol., B 36, 03F102 (2018).
- ²⁶C. J. Gu, F. A. Stevie, C. J. Hitzman, Y. N. Saripalli, M. Johnson, and D. P. Griffis, Appl. Surf. Sci. 252, 7228 (2006).
- ²⁷B. B. Haidet, B. Sarkar, P. Reddy, I. Bryan, Z. Bryan, R. Kirste, R. Collazo, and Z. Sitar, Jpn. J. Appl. Phys., Part 1 56, 100302 (2017).
- 28K. Seeger, Semiconductor Physics: An Introduction (Springer Science & Business Media, 2013).
- ²⁹M. E. Levinshtein, S. L. Rumyantsev, and M. S. Shur, Properties of Advanced Semiconductor Materials: GaN, AIN, InN, BN, SiC, SiGe (John Wiley & Sons, 2001).
- ³⁰S. F. Chichibu, H. Miyake, Y. Ishikawa, M. Tashiro, T. Ohtomo, K. Furusawa, K. Hazu, K. Hiramatsu, and A. Uedono, J. Appl. Phys. 113, 213506 (2013).
- ³¹S. Washiyama, P. Reddy, B. Sarkar, M. H. Breckenridge, Q. Guo, P. Bagheri, A. Klump, R. Kirste, J. Tweedie, S. Mita, Z. Sitar, and R. Collazo, J. Appl. Phys. 127, 105702 (2020).